Available online at www.sciencedirect.com
SCIENCE DIRECT
Catalysis Today 114 (2006) 94–101
CATALYSIS TODAY
www.elsevier.com/locate/cattod

Nitrogen release from a NO_x storage and reduction catalyst

R.G. Tonkyn *, R.S. Disselkamp, C.H.F. Peden

Institute for Interfacial Catalysis, Pacific Northwest National Laboratory, P.O. Box 999, MS K8-88, Richland, WA 99352, USA

Available online 27 March 2006

Abstract

In a NO_x storage and reduction (NSR) catalyst, the release and reduction of NO_x occurs over a very short period. The speed of the NO_x release and reduction creates difficulties in analyzing the chemistry using normal analytical techniques, which are typically better suited to slower, steady-state studies. We have investigated the time dependence of NO, NO_2, NH_3, N_2O and N_2 released by an NSR catalyst using a combination of FT-IR and gas chromatographic techniques. Nitrogen was detected with the GC by using He rather than N_2 as the background gas. The FT-IR was used not only to monitor NO, NO_2, NH_3 and N_2O, but also to establish cycle-to-cycle reproducibility. Under these conditions we used the GC to sample the effluent at multiple times over many lean–rich cycles. To the extent that the chemistry was truly periodic and reproducible, we obtained the time dependence of the release of nitrogen after the lean-to-rich transition. Similar information was obtained for O_2, H_2 and N_2O. Combining the FT-IR and GC data, we obtained good cycle averaged nitrogen balances, indicating that all the major products were accounted for.

Keywords: NO_x trap; Storage/reduction; Nitrogen balance; Lean–rich cycling; Diesel emissions

1. Introduction

Due to their inherently higher fuel efficiency, the expanded use of diesel engines in automobiles and light duty trucks would result in a significant reduction in CO_2 emissions [1]. Unfortunately it has proven quite a challenge to reduce the NO_x emissions from diesel engines to acceptable levels. The strongly oxidative environment of lean-burn engine exhaust is a difficult one in which to chemically reduce NO and NO_2 to N_2. One promising approach is the use of NO_x storage and reduction (NSR) catalysts, often also called lean-NO_x trap (LNT) catalysts [2–4]. These catalysts very efficiently store NO_x under lean conditions, typically as a nitrate. Under rich conditions, the nitrate is readily reduced to N_2 leaving the catalyst ready to store NO_x again once lean conditions are re-established. One strategy for utilizing the NSR approach is to periodically operate the engine under both lean (i.e., excess oxygen) and rich (i.e., excess fuel) conditions. The lean operation period should be much longer than the rich one in order to take advantage of the natural ''lean-burn'' condition of a diesel engine.

The lean–rich cycling times are dictated by the lean cycle NO_x storage capacity and the rich cycle reduction rate. Careful optimization of the timing and length of the rich period will be necessary in order to minimize the fuel penalty while maintaining the requisite NO_x conversion efficiency. In practice the engine management will likely be very complicated, given the wide range of operating conditions to be expected for everyday driving. One important piece of information is the time evolution of nitrogen-containing species during the lean and especially the rich cycle. How this depends on variables such as the temperature, reductant identity, humidity, CO_2 concentration, and the space velocity is vital information required to develop any engine management strategy.

During the rich cycle, there is a very short burst of activity accompanied by large composition changes that make the chemistry difficult to follow. Furthermore, because nitrogen is the majority species in air, it is virtually impossible to detect and quantify N_2 formation during ordinary operation. Generally, nitrogen formation is inferred by the loss of NO_x and the inability to detect other logical nitrogen-containing products [5–7]. However, this type of inference is not completely satisfying, and gives little or no time-dependent information. Our approach to this problem is to synthesize simplified synthetic exhaust in which He has replaced atmospheric N_2. In addition, we take advantage of the periodic nature of NSR catalyst operation to sample the exhaust gases at many points

* Corresponding author. Tel.: +1 509 376 8817; fax: +1 509 376 6066.
E-mail address: rg.tonkyn@pnl.gov (R.G. Tonkyn).

0920-5861/$ – see front matter
doi:10.1016/j.cattod.2006.02.005

over a series of cycles. As long as the chemistry is truly periodic, under these conditions the time dependence of the formation of N_2 can readily be established.

For the initial experiments reported here, we simplified the chemistry as much as possible, adding only NO_x, H_2 and O_2 to the background He flow. As has been pointed out [8], the lack of CO_2 and excess water is an unrealistic condition for diesel exhaust. However, both the storage and reduction chemistry of NSR catalysts is qualitatively, if not quantitatively, quite similar with or without these components. In future experiments, the effects of H_2O and CO_2 will be examined.

2. Experimental

Our experimental apparatus contains a gas handling system, a temperature controlled quartz reactor containing our monolith catalyst, and an FT-IR and micro-GC for effluent gas analysis. The gas handling system uses pure or mixed gases (i.e., He, O_2, H_2, and 0.5% NO or NO_2 in He) to form three separate gas streams, labeled the main, lean and rich flows. For the experiments described here, the main flow consisted of a fixed concentration of NO or NO_2 in helium. Other gases (e.g., CO_2, SO_2, and/or H_2O) could be added to this flow as well, but were not included for our first experiments reported here. The lean and rich flows consisted of either oxygen or hydrogen mixed with helium at the appropriate concentration. Two computer controlled three-way solenoid valves were simultaneously switched such that one of these mixtures was added to the main flow upstream of the catalytic reactor while the other was directed to the exhaust. Therefore, during the rich period no oxygen was present and during the lean period no hydrogen was present. By using equal volumetric flow rates of the rich and lean gases, the inlet NO_x concentration remained constant throughout the experiment. The gas manifold included a manual bypass valve used to set up and check the inlet gas concentrations.

Our catalytic reactor consisted of a 2.5 cm OD × 2.2 cm ID × 40 cm long quartz tube adapted to 0.64 cm diameter glass tubing on both the inlet and outlet ends. We added a coarse glass frit near the inlet end so that loosely packed glass beads could be inserted upstream of the catalyst to enhance gas mixing and temperature equilibration. The reactor's large open end was adapted to a threaded glass connector, and a threaded Teflon plug used to seal the reactor. The plug was removed to load or unload the catalyst, and had a centered, threaded hole used to insert a type-K thermocouple into the reactor right up against the downstream end of the catalyst. A small monolithic piece (∼2.1 cm diameter × 2.1 cm long, ∼7 cm^3) of a degreened (16 h in air at 700 °C in 10% H_2O) commercial lean NO_x trap catalyst manufactured by Umicore was sealed against the walls of the reactor by wrapping with fiberglass string and then placed near the outlet end of the reactor. The entire reactor was housed inside a 12 in. temperature programmable horizontal furnace (Lindberg/Blue). The furnace was temperature controlled using its own external thermocouple, but we report here the actual temperatures recorded inside the reactor at the outlet end of the catalyst.

The Umicore catalyst in many ways resembles a three-way catalyst with added barium for storage. This catalyst was supplied to us by Oak Ridge National Laboratory and is being used in several laboratories as a benchmark NSR catalyst. It contains the precious metals Pt, Pd and Rh (in descending quantities), added ceria and zirconia (for oxygen storage) and BaO for NO_x storage. The barium loading is 20 wt.% as BaO on Al_2O_3, and the targeted precious metal loading was 100 g/ft.^{3} of Pt/Pd/Rh in a 9:3:1 ratio.

After exiting the reactor, the gas flow was directed through mildly heated stainless steel tubing (∼50 °C) to the FT-IR or the micro-GC for analysis. The FT-IR (Nicolet Magna 560) was equipped with a 2 m gas cell held at 50 °C and a liquid nitrogen cooled MCT detector. The gas cell had a volume of 200 cm^3, which was equal to approximately 5 s of flow at 2 standard liters per minute. The ultimate time response of the FT-IR was therefore limited by the gas turnover time in the cell. We utilized the OMNIC software package to obtain and quantify spectra (2–3 scans at 0.5 cm^{-1} resolution) every 3–4 s. For most gases, we obtained standard calibration spectra on site using gas mixtures with known concentrations. For ammonia, we obtained a 1 ppm-meter standard spectrum, also taken at 50 °C, from the PNNL spectral library [9]. Based on calibration experiments using He dilution, we can say that the relative accuracy of our method is quite good. The absolute accuracy is harder to quantify due to the combined effects of errors in the calibration standards, the various flow rates, and any interference effects not correctly compensated for. However, the consistent and nearly complete nitrogen balances we obtained under a number of different conditions suggests the absolute accuracies were acceptable.

Our micro-GC (MTI analytical Quad series) was equipped with both a 10 m 5 Å molecular sieve column held at 60 °C and a 6 m Poroplot U column held at 50 °C. The former was used to detect H_2, O_2, and N_2, while the latter was utilized to measure N_2O. Under these conditions, approximately 65 s was required to elute all the gases present, which determined the shortest possible time between injections. Since the GC sampled the flow at only one instant during a cycle, it was necessary to control the lean-to-rich transition with respect to the GC injection over a series of identical cycles. This was accomplished by letting the GC free run at a predetermined injection rate and adjusting the lean-to-rich transition time accordingly. Although we did not control the injection time externally, we were able to record the injection time for comparison with the computer controlled lean-to-rich transition. By programming the total lean–rich cycle period to be slightly shorter than the GC repeat time, we were able to sample gas over the entire rich period. The number of sample points (i.e., lean–rich cycles) required to measure through the entire rich period was determined by the length of the rich period in combination with the difference between the lean–rich cycle time and the GC repeat time. Once we knew the transit time from the solenoid valve to the GC inlet (approximately 6 s) we could adjust the initial parameters such that the first few injections sampled gas from late in the

lean period, with each subsequent injection falling relatively later in the cycle. With enough lean–rich cycles, we were able to then sample across the entire rich period and beyond. Assuming consistent cycle-to-cycle chemistry, the time resolution using this method was determined by the step size we chose. As a matter of practicality we chose time-steps of 0.3 s for the shortest rich periods, increasing to 2 s for the longest periods.

A typical experiment was run as follows. By bypassing the catalyst, the inlet NO_x concentration for both the rich and lean flow mixtures was determined. The gas was then passed over the catalyst and a series of lean–rich cycles were run. Using the FT-IR to make nearly real-time measurements of the NO, NO_2, N_2O, H_2O and NH_3 concentrations, we waited until reproducible lean–rich cycles were obtained, which typically took between 10 and 60 min. We had to wait until both the chemistry and the temperature stabilized, since a significant amount of heat was evolved during the rich period. If necessary, the furnace set point was adjusted to obtain the desired temperature. Once we were satisfied that the chemistry and temperature were stable, we bypassed the FT-IR and began the GC experiments. The first few injections were timed to sample gas late in the lean period, and typically showed only O_2. Eventually the GC sampled gas from the rich phase, and N_2 and N_2O appeared as oxygen disappeared. In longer rich cycles, we detected NH_3 and H_2 as well. The data were collected over the entire rich period and into the start of the following lean period. We quantified the data by comparing the N_2 detected by the GC with the other species measured on the FT-IR during one cycle just prior to the beginning of the GC experiments.

Unless otherwise noted, our experimental conditions were as follows. The total flow was two standard liters per minute over a 7 cm^3 coated catalyst brick for a calculated gas-hourly space velocity of $\sim$17 000 h^{-1}. The input NO_x concentration was fixed at 280 ppm of NO during both cycles. Lean flow included 4% oxygen, while rich flow contained 1.3% hydrogen. The catalyst temperature was between 250 and 260 °C.

3. Results and discussion

3.1. Chemistry under 'steady-state' rich conditions

The operation of an NSR catalyst requires that the majority of the time NO_x is simply stored, with all the important NO_x reduction chemistry occurring during a very short rich period. As a starting point, the 'steady-state' chemistry of the catalyst under rich conditions is of interest. Because the catalyst formulation can be described as a typical ''three-way'' catalyst with additional BaO for NO_x storage capacity, this period can be regarded as steady-state ''three-way''-like NO_x reduction. With our simplified gas mixture the result is straightforward. At 255 °C, once all the stored NO_x and oxygen has been depleted, H_2 reduces NO in the input gas to both NH_3 ($\sim$75% of input N) and N_2 ($\sim$25%), producing water as well. No NO_x or N_2O was observed at all during this period. The nitrogen balance indicated no other major species were formed. The reactions forming NH_3 and N_2 can be written in balanced form as follows:

$$NO + (5/2)H_2 \Leftrightarrow NH_3 + H_2O \quad (1)$$

$$2NO + 2H_2 \Leftrightarrow N_2 + 2H_2O \quad (2)$$

Since the second reaction requires two NO molecules to react while the first only one, we ran a series of experiments measuring the steady-state N_2 and NH_3 concentrations for a range of NO concentrations between 80 and 1100 ppm. For these experiments the H_2 concentration was fixed at 1.3%. We observed no change in the NH_3:N_2 branching ratio, which remained at 3:1 over the entire range. Apparently whatever change in the NO surface coverage occurred over this concentration range had no effect on the relative reaction rates. While it is possible that this range of NO concentrations was insufficient to significantly alter the 'steady-state' catalyst surface concentrations, another plausible explanation is that the two reactions occur on different sites (e.g. Pt versus Rh or Pd) and are therefore independent of each other.

We ran a single experiment at 270 ppm input NO_x as NO_2 rather than NO. The result was very similar. At 253 °C, we detected only N_2, NH_3 and water. In this case, we measured 70% conversion of NO_2 to NH_3, with the remainder forming N_2. The measured water was twice the inlet NO_2 concentration, as expected. Again the nitrogen balance was excellent.

3.2. Chemistry under lean conditions

In Fig. 1 we show a single, long lean period taken after the stored NO_x from prior lean periods had been fully removed by reduction with H_2. As soon as we switched to lean conditions, NH_3 disappeared, and no gas-phase N-containing species were observed for approximately 20 min. Eventually NO broke through the catalyst, reached a maximum at about the time NO_2 appeared, and then declined back to a nearly constant value. Qualitatively similar NO_x breakthrough curves have been reported elsewhere [10–12]. The long-term NO_x breakthrough

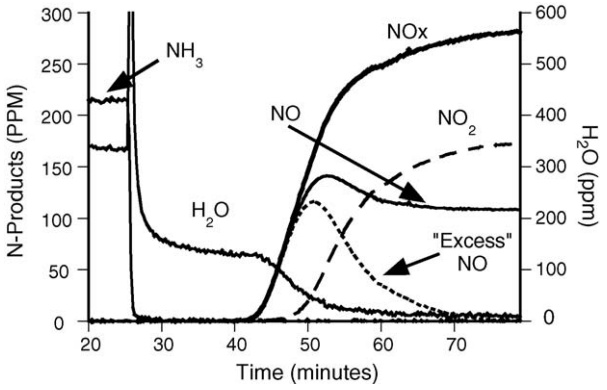

Fig. 1. N-containing products (left axis) and water (right axis) observed during a long lean period. The input gas composition was 4% O_2, 270 ppm NO with the balance He. The catalyst out temperature was 255 °C. The reactor was pre-treated with a rich feed of 1.3% H_2, 270 ppm NO and balance He. The ''excess'' NO represents NO out in excess of the amount predicted by the steady-state ratio of NO to NO_2.

simply reflects NO oxidation kinetics on the precious metals in the catalyst as the NO_x storage capacity of the NSR is reached [13,14]. No steady-state NO_x conversion was observed under lean conditions. At 255 °C and with 4% oxygen, thermodynamic equilibrium favors more NO_2 than we observe, so this must be considered a 'steady-state' rather than equilibrium condition, and the rate of NO oxidation kinetically controlling under these conditions. We note that within this lean cycle, the H_2O concentration dropped to a nearly steady value until NO started to break through the catalyst. At this point, the H_2O concentration dropped fairly rapidly to zero. The concentration of H_2O was approximately one half that of the input NO for the bulk of the time that NO_x was completely removed from the inlet stream via storage. This result suggests that H_2O, not present in the input gas mixtures, was displaced from barium storage sites that were converted to $Ba(OH)_2$ rather than BaO during the long period of soaking in $H_2 + NO_2$. The water dropped to zero at about the same time NO appeared, consistent with NO production as the last step of NO_x storage.

Our NO_x adsorption data is consistent with the stepwise adsorption of NO_2 at the barium sites, with the final process being an oxidation by NO_2 that releases NO. The overall stoichiometry for NO_2 storage has been suggested to be the following [11,15,16]:

$$(1/2)O_2 + NO + Pt \Leftrightarrow NO_2 + Pt \quad (3)$$

$$3NO_2 + BaO \Leftrightarrow Ba(NO_3)_2 + NO \quad (4)$$

Our data is consistent with this process. The input NO is oxidized to NO_2 at a precious metal site, but the reverse reaction is interrupted by rapid adsorption of NO_2 at Ba containing storage sites. Initially, any NO regenerated by the last adsorption step is re-oxidized and taken up further down the catalyst bed. As the catalyst fills up, the final adsorption step occurs closer to the catalyst outlet, until eventually NO escapes. We observe a "burst" of NO out which settles down as the storage sites are completely filled. From the data shown, we calculate the storage capacity of our catalyst under these conditions to be ~650 μmol of NO_x, or ~90 mol/m^3. Of course this value will likely vary with changes in reaction conditions such as temperature, gas composition, space velocity and the like. The storage capacity has been reported to drop with the addition of H_2O and CO_2, although the general form of the NO_x adsorption trace is still quite similar [8,11]. In Fig. 1, we include a trace showing the amount of NO in excess of the steady-state amount expected, as calculated from the NO_2 trace and the final steady-state ratio of NO to NO_2. Integration of this trace indicates the excess NO released amounts to ~20% of the NO_x stored. The fact that this is less than predicted by Eq. (4) above is consistent with the idea that much of the NO initially formed near the front is re-oxidized and reused further down the catalyst. An alternative hypothesis is that the lower than predicted NO recovered indicates the presence of two types of storage sites, one of which requires NO_2 for the final oxidation to $Ba(NO_3)_2$, and one of which can store NO_2 as a nitrate using O_2 as the oxidant [11]. The latter sites would not produce any product NO. Our data cannot distinguish these possibilities.

The exact same experiment run with 270 ppm NO_2 rather than NO yielded very similar results. After reaching 'steady-state' under rich conditions, switching to lean flow caused complete storage of all input NO_2 for ~20 min. The first NO_x out was in the form of NO, but NO peaked as NO_2 appeared, and the final condition reflected the concentrations of NO_2 and NO obtained by the reverse NO oxidation reaction on the precious metal. In this case, we had more NO_2 than predicted by thermodynamics, again indicating that the reactions are not fast enough to reach equilibrium at 17 000 h^{-1} over what is likely at least partially oxidized precious-metal catalyst components.

3.3. Short rich period

In Fig. 2a, we show FT-IR data taken over one full cycle (67 + 3 s, lean + rich) after the system had been allowed to stabilize for 35 min with the reproducibility of the FT-IR data verified for several lean–rich cycles. As mentioned above, due to the volume of the FT-IR cell the inherent time resolution of the data is significantly longer than the actual rich period in this case. At the end of the previous lean period (left edge of the figure) both NO and NO_2 were present in significant amounts. Upon switching to the rich feed, we observed an immediate pulse of NO and N_2O, a pulse of NO_2 noticeably delayed in

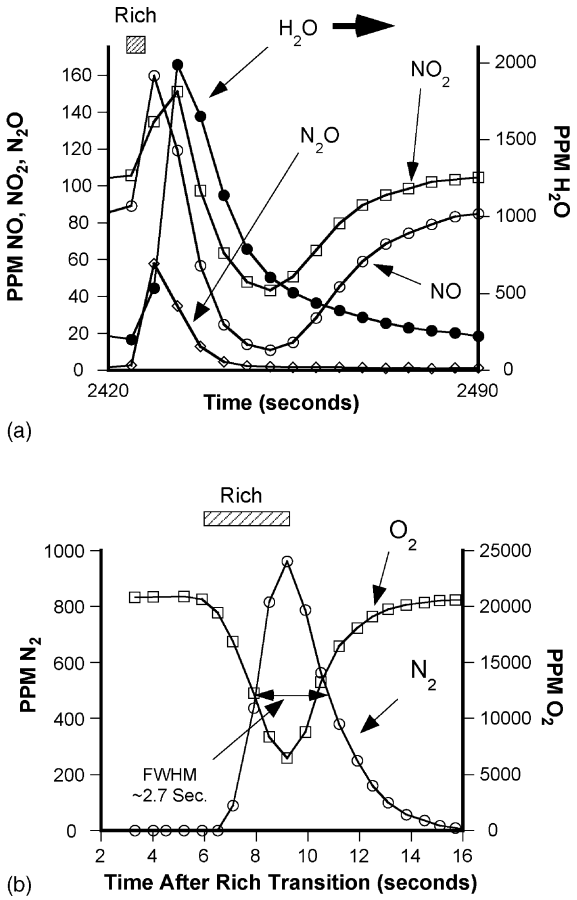

Fig. 2. Products detected by FT-IR (a) and GC (b) for a lean/rich cycle of 67/3 s. The box labeled Rich at the top of each plot represents the width of the rich period. Rich flow: 1.3% H_2, 270 ppm NO, balance He. Lean flow: 4% O_2, 270 ppm NO, balance He.

time from the NO and N_2O ones, and a quite large burst of H_2O perhaps even further delayed in time. Neither the NO nor the NO_2 concentrations dropped to zero at any point during the cycle. Despite the evident saturation of the NO_x storage capacity, the release of the majority of NO_x during the lean period as NO_2 indicates that NO oxidation was still occurring. Both H_2O and NO_2 would be expected to adsorb more strongly to the catalyst (and tubing walls), which might at least partially explain their later appearance. The delayed appearance could also result from a slower formation step and/or different precursors, thus reflecting aspects of the reaction mechanisms during the rich phase—aspects we will explore further in future experiments.

Once the FT-IR indicated that reproducible lean–rich cycles had been attained, we began sampling the flow with the gas chromatograph. The resulting measurement of O_2 and N_2 is shown in Fig. 2b, with each set of two data points at a particular time obtained from a single lean–rich cycle. As can be seen, the excellent time resolution and smooth rise and fall of detected N_2 is another indication that the chemistry was stable over many cycles. The width of the N_2 signal is consistent with a 3 s rich period, with the somewhat slow decay due to a slow sweeping out of nitrogen from the catalyst volume. We note that in the lean mix the oxygen signal was saturated due to the high sensitivity scale of the GC detector required to detect N_2 that was, of course, present at much lower concentrations. However as the oxygen concentration fell, it did drop into the linear response region. Over a 3 s rich cycle oxygen never dropped completely to zero. In fact, even at its lowest concentration the oxygen concentration remained well in excess of the input NO_x. Although the catalyst is expected to store some oxygen, this result is most likely due to a slow sweeping out of the catalyst. Experiments with added N_2 in the rich feed (and no NO_x in the main feed) indicated that both N_2 and O_2 have similar time behavior when switched on and off and passed through the catalyst. Since we do not expect nitrogen to adsorb, we attribute the slow decay of oxygen mainly to mixing and diffusion effects. Any effect due to oxygen storage on ceria would probably be too subtle for us to measure under these conditions.

The raw data from both the FT-IR and GC experiments was integrated over the entire cycle (in units of ppm s) and the result converted to μmol utilizing the flow rate and the ideal gas law. Table 1 lists the results for 3 consecutive cycles, including the cycle shown in Fig. 2a. The steady-state nature of the chemistry is quite apparent, which gives us confidence that sampling the gas for the GC measurements at different points across many lean–rich cycles is a reasonable strategy. Table 1 also includes the measured N_2, which when combined with the FT-IR data indicates that ~95% of the input N was recovered. However, only one third of the input NO_x was reduced to nitrogen under these conditions. The amount of water produced was significantly greater than possible for the reduction of NO_2 to N_2 and N_2O observed, meaning that most of the water was formed via H_2 reduction of oxygen, probably stored on the ceria–zirconia component of the NSR catalyst.

Table 1
Products detected over consecutive cycles

	#1	#2	#3	% NO_x
NO (μmol)	5.7	5.7	5. 7	21
NO_2 (μmol)	9.3	9.3	9.3	34
N_2O (μmol)	0.84	0.84	0.84	6
Sum (μmol N)	16.7	16.7	16.7	61
H_2O (μmol)	65	65	65	
N_2 (μmol)	4.6			34

3.4. Long rich period

Fig. 3 shows a similar set of FT-IR(a) and GC(b) data for the case of a 67–20 s lean–rich cycle. In this case NO and NO_2 are not plotted because no NO_x was detected at any point during the lean–rich cycle. Upon switching to rich conditions, on the FT-IR we observed an immediate pulse of N_2O followed by a distinctly slower appearance of H_2O, and after 10 s or so, the appearance of NH_3 as well. On the GC, upon switching to rich conditions we saw a rapid rise and fall of N_2, with an FWHM of ~5 s. The nitrogen signal leveled off to a small but non-zero value, consistent with our discussion above concerning 'steady-state' "three-way"-like catalysis. Fig. 3b also shows that approximately 10 s into the rich cycle oxygen essentially disappeared and hydrogen appeared. Comparing the GC and FT-IR traces we

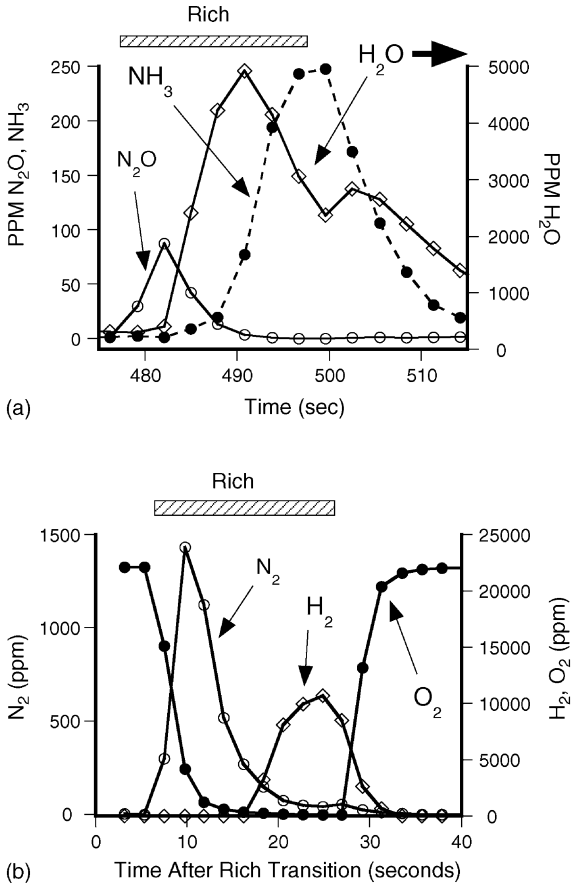

Fig. 3. Products detected by FT-IR (a) and GC (b) for a lean/rich cycle of 67/20 s. The box labeled rich at the top of each plot represents the width of the rich period. Rich flow: 1.3% H_2, 270 ppm NO, balance He. Lean flow: 4% O_2, 270 ppm NO, balance He.

note that the H_2 and NH_3 signals were very similar. Both products appeared after gas-phase oxygen was gone, and rose toward their 'steady-state' values until the switch back to lean conditions occurred. We also note that a large amount of H_2O was produced as long as excess oxygen was present. The H_2O concentration peaked approximately 10 s into the rich cycle, then dropped smoothly until the beginning of the subsequent lean period. At that point a small upward spike in the H_2O signal was observed, presumably due to the reaction of O_2 with H_2 left over on the catalyst from the rich flow.

Evidently N_2O and N_2 are formed immediately after the lean-to-rich transition and are the primary N-containing products from stored NO_x. The formation of NH_3 occurred later, presumably from reactions of the input NO with H_2 on precious metal sites after gas-phase oxygen was gone. The absolute concentration of N_2 observed confirms that it arises from stored NO_x. However, the N_2O concentrations are low enough that we cannot determine from our data whether the production of N_2O involved only stored NO_x. In the future we plan to determine the effect, if any, that varying the concentration of NO_x in the rich phase has on the production of N_2O and N_2.

3.5. Varying the rich period

We ran a series of experiments in precisely the same manner, but with varying rich periods. We collected data for a 67-s lean period followed by rich periods ranging from 2 to 20 s. Fig. 4a shows the GC-measured N_2 production data for selected rich periods, and Fig. 4b summarizes the entire data set in terms of % NO_x conversion. Table 2 contains the detailed results illustrated in Fig. 4b. In the table we define the "% NO_x conversion" as the net loss of NO_x, regardless of the product formed.

Our results can be summarized as follows. As the rich period increased from 2 to 6 s, the amount of NO_x surviving the catalyst dropped rapidly to zero, where it remained for all longer rich period cycles. Over the same range the amount of N_2 produced increased rapidly, and then leveled off, with essentially no further increase at rich times longer than ~5–6 s. The amount of N_2O went up from 2 to 5 s rich, and then was level or perhaps tailed off slightly over the rest of the range. Ammonia appeared at measurable levels only in cycles with 8 s or longer rich periods, and monotonically increased with the length of the rich period. We discuss the effects of the length of the rich period on the individual products below.

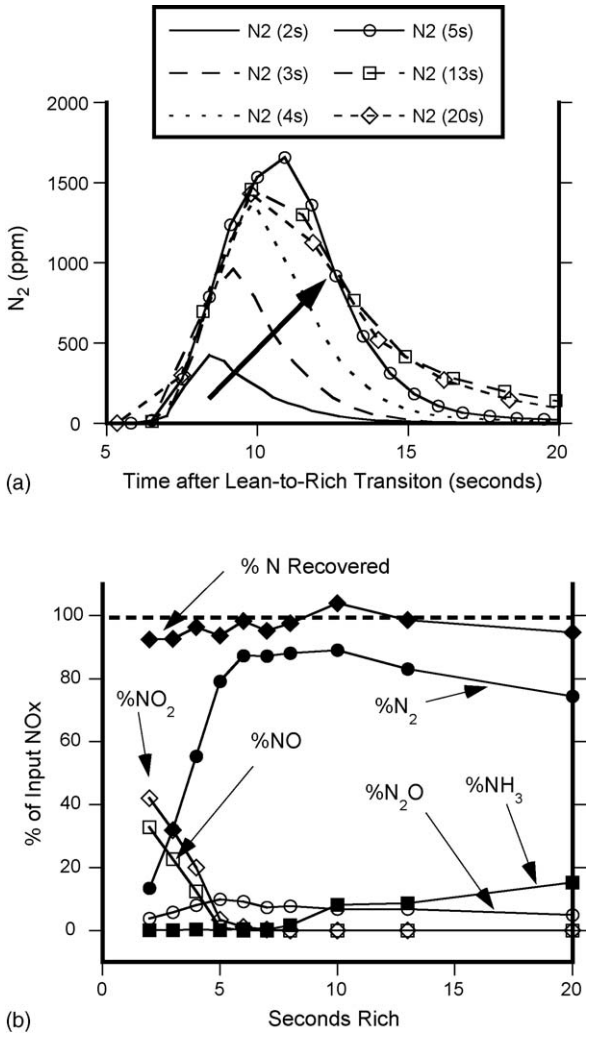

Fig. 4. Results for a series of lean/rich cycle times, with the lean period fixed at 67 s and the rich time varied from 2 to 20 s. (a) Shows the time dependence of N_2 production for selected rich periods; (b) indicates the complete results for N-containing products.

3.6. Production of N_2O

For most of the experiments described here, we utilized the FT-IR to analyze for N_2O, which appeared to arise immediately upon addition of hydrogen. However since the FT-IR and the GC had significantly different inherent time responses, we ran

Table 2
Integrated results for 2–20 s rich periods

	Seconds rich									
	2	3	4	5	6	7	8	10	13	20
N_2 (μmol N out)	3.8	9.3	16	24	26	26	27	28	27	26
NO (μmol out)	9.3	6.6	3.7	0.3	0	0	0	0	0	0
NO_2 (μmol out)	12	9.3	5.9	1	0.4	0.1	0	0	0	0
N_2O (μmol N out)	1.1	1.7	2.4	3.0	2.8	2.2	2.4	2.1	2.2	1.8
NH_3 (μmol out)	0.1	0.1	0.1	0	0.2	0.1	0.5	2.6	2.9	5.5
% NO_x conversion	25	45	67	95	99	100	100	100	100	100
% N balance	92	93	97	95	98	95	98	104	98	95
H_2O (μmol out)	48	65	78	91	103	114	125	145	146	182

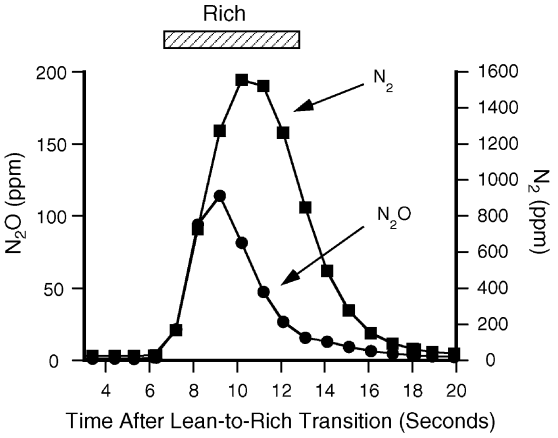

Fig. 5. Comparison of N_2 and N_2O production during a 67/6 s lean/rich cycle. Both products were detected by GC. The box labeled Rich at the top the plot represents the width of the rich period. Rich flow: 1.3% H_2, 270 ppm NO, balance He. Lean flow: 4% O_2, 270 ppm NO, balance He.

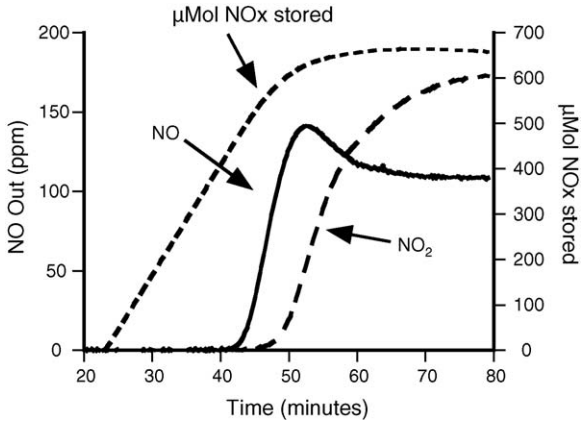

Fig. 6. NO_x out and NO_x stored vs. time during a long lean period. This is taken from the same experimental data shown in Fig. 1. The input gas composition was 4% O_2, 270 ppm NO with the balance He. The reactor was pretreated with a rich feed of 1.3% H_2, 270 ppm NO and balance He.

one experiment where we measured N_2O using a second column in the GC. Fig. 5 shows the result for a 6 s rich/67 s lean cycle. Clearly N_2O is formed coincidently with N_2 in the initial stage of the rich period, but is depleted much more quickly. Since the time behavior of N_2O and NO as measured by the FT-IR were nearly identical, the same can be said for the pulse of NO detected when rich cycles were less than or equal to ~5–6 s. As we see in Table 2, although the NO signal dropped rapidly to zero for longer rich cycles, a small but persistent N_2O signal could not be avoided under these conditions. For longer rich cycles, the N_2O appearance was identical to that seen in shorter cycles, namely a short burst that appeared immediately after the lean-to-rich transition.

The rapid and evidently unavoidable appearance and disappearance of N_2O suggests that, in every case, a relatively small fraction of the stored NO_x is ''primed'' to form N_2O once oxygen is removed. The fact that the N_2O formation is at best only very weakly linked to the length of the rich period is consistent with it being formed on the precious metal rather than the NO_x storage sites. One plausible explanation is that as H_2 rapidly cleanses O from Pt, the $N + NO \Leftrightarrow N_2O$ reaction occurs. At later times, the NO surface concentrations on the precious metals may be small compared to H-atom and N-atom concentrations so N_2 and NH_3 become the dominant N-containing products of NO_x reduction. We note that the amount of N_2O formed never exceeds the amount of NO input during the rich cycle, so it is possible the NO required for the above reaction is NO(g) rather than NO from stored NO_x, although this remains ambiguous pending further experiments.

3.7. Release of NOx

We only observed NO_x out after the lean-to-rich transition in cases where both NO and NO_2 were also present at measurable concentrations during the lean phase. In every one of these cases, NO_x out was significant at all times during the cycle. Obviously in these cases, the rich period was too short to remove all of the stored NO_x. However, even immediately after the ''partial'' cleaning the catalyst was unable to take up all of the input NO_x. By the same token, whenever the rich period was long enough to 'clean' the catalyst of stored NO_x, NO_x out was zero for the entire cycle.

In some sense, this NO_x release behavior is a consequence of our experimental procedure. In particular, we waited until steady-state had been reached before collecting any of the cycle data shown. We began with a reduced catalyst and ran consecutive cycles until we reached consistent behavior for consecutive lean–rich cycles. Consider all cases where NO and NO_2 were observed during the lean cycle. Since the rich phase was too short to fully 'clean' the catalyst, each successive cycle left more and more NO_x behind. This process continued until the lean NO_x storage rate slowed down enough that the NO_x removed during the rich phase equaled the amount stored during the lean stage. In Fig. 6 we show the long lean period data recast in terms of µmol of NO_x stored versus time. The rate of storage, or derivative of the trace, is constant right up until NO appears in the effluent, when it slows considerably. Whenever we studied conditions leading to a non-zero NO_x output at the end of the lean period, we had a nearly full catalyst. In these cases, NO_x storage was slow after switching back to lean flow because the catalyst was still quite full; therefore, NO and NO_2 appear immediately. While it would presumably be possible to construct a cycle which under steady-state conditions that included lean NO_x breakthrough and full rich cycle cleaning, under the conditions illustrated in Fig. 6 the cycle time would be extremely long and, thus, experimentally impractical. Under other operating conditions (e.g., higher temperature, higher NO_x concentration or lower catalyst loading), such a cycle might be more conveniently obtained and probed experimentally.

3.8. N_2 and NH_3 production

The traces shown in Fig. 4a make it immediately apparent those conditions that lead to optimum nitrogen production. The formation of nitrogen was obviously reductant limited up to rich cycles of 5 s or so. However, lengthening the rich period beyond 5

or 6 s did not significantly increase the amount of nitrogen produced, indicating that at the optimum point, the gas-phase concentration of reductant and the amount of stored NO_x were well balanced. This result is valid only for the precise conditions we used. Varying the hydrogen concentration could conceivably change the rich time required for optimum NO_x reduction, although we have not addressed that issue to date. The addition of H_2O and CO_2 will doubtless change the optimum conditions as well. It is especially notable that the reduction of stored NO_x yields primarily N_2, with only small amounts of N_2O formed. Importantly, ammonia was not observed at all during an optimized lean–rich cycle, but only appeared during very long rich periods. This implies that the H-atom surface concentrations on the precious metal are relatively small until the stored NO_x is reduced. The appearance of NH_3 indicates no further gains can be obtained by further lengthening the rich period.

4. Conclusions

The reduction of stored NO_x by H_2 in a commercial NSR catalyst has been shown to produce mainly N_2 with smaller quantities of N_2O. For insufficiently long rich periods, the adsorbed NO_x builds up until the lean-cycle NO_x storage is drastically reduced, degrading the overall performance significantly. Under these conditions, the catalyst never fully removes stored NO_x, and NO and NO_2 are observed throughout the entire lean–rich cycle. During overly long rich periods, NO_x is never observed but, unfortunately, NH_3 is. Compared to an optimized rich cycle length, similar amounts of N_2 are produced early in the rich period, but its production drops off significantly once the stored NO_x is depleted. The reduction of input NO takes place then and favors NH_3 production over N_2 production by a 3:1 margin over a wide range of NO concentrations. The appearance of ammonia is an excellent indication that nitrogen production from stored NO_x is complete, and that the optimal rich period has been reached or exceeded. Importantly, the proper choice of the rich period length prevented the production of significant amounts of NH_3 altogether. Under our conditions, a small but noticeable amount of N_2O was unavoidably produced.

Acknowledgments

We acknowledge the financial support from the U.S. Department of Energy (DOE), Office of Freedom Car and Vehicle Technologies. The experiments were performed in the Environmental Molecular Sciences Laboratory (EMSL) at Pacific Northwest National Laboratory (PNNL). The EMSL is a national scientific user facility and supported by the US DOE's Office of Biological and Environmental Research. PNNL is a multi-program national laboratory operated for the U.S. Department of Energy by Battelle Memorial Institute under contract number DE-AC06-76RLO 1830.

References

[1] R.M. Heck, R.J. Farrauto, Catalytic Air Pollution Control, Van Nostrund Reinhold, New York, 1995.
[2] W. Bogner, M. Kramer, B. Krutzsch, S. Pischinger, D. Voigtlander, G. Wenninger, F. Wirbeleit, M.S. Brogan, R.J. Brisley, D.E. Webster, Appl. Catal. B: Environ. 7 (1995) 153.
[3] N. Takahashi, H. Shinjoh, T. Iijima, T. Suzuki, K. Yamazaki, K. Yokota, H. Suzuki, N. Niyoshi, S. Matsumoto, S. Tanizawa, S. Tanaka, T. Tateishi, K. Kashara, Catal. Today 27 (1996) 63.
[4] W.S. Epling, L.E. Campbell, A. Yezerets, N.W. Currier, J.E. Parks, Catal. Rev. Sci. Eng. 46 (2004) 163.
[5] E. Fridell, M. Skoglundh, B. Westerberg, S. Johansson, G. Smedler, J. Catal. 183 (1999) 196.
[6] Z.Q. Liu, J.A. Anderson, J. Catal. 224 (2004) 18.
[7] K.S. Kabin, R.L. Muncrief, M.P. Harold, Catal. Today 96 (2004) 79.
[8] W.S. Epling, G.C. Campbell, J.E. Parks, Catal. Lett. 90 (2003) 45.
[9] S.W. Sharpe, T.J. Johnson, R.L. Sams, P.M. Chu, G.C. Rhoderick, P.A. Johnson, Appl. Spectrosc. 58 (2004) 1453.
[10] P. Broqvist, H. Gronbeck, E. Fridell, I. Panas, Catal. Today 96 (2004) 71.
[11] W.S. Epling, J.E. Parks, G.C. Campbell, A. Yezerets, N.W. Currier, L.E. Campbell, Catal. Today 96 (2004) 21.
[12] F. Prinetto, G. Ghiotti, I. Nova, L. Castoldi, L. Lietti, E. Tronconi, P. Forzatti, Phys. Chem. Chem. Phys. 5 (2003) 4428.
[13] S.S. Mulla, N. Chen, W.N. Delgass, W.S. Epling, F.H. Ribeiro, Catal. Lett. 100 (2005) 267.
[14] L. Olsson, B. Westerberg, H. Persson, E. Fridell, M. Skoglundh, B. Andersson, J. Phys. Chem. B 103 (1999) 10433.
[15] N.W. Cant, M.J. Patterson, Catal. Today 73 (2002) 271.
[16] J. Depres, M. Koebel, O. Krocher, M. Elsener, A. Wokaun, Appl. Catal. B: Environ. 43 (2003) 389.